An Exactly Solvable Ogston Model of Gel Electrophoresis. 7. Diffusion and Mobility of Hard Spherical Particles in Three-Dimensional Gels

Jean-François Mercier and Gary W. Slater*

University of Ottawa, 150 Louis-Pasteur, Ottawa, Ontario K1N 6N5, Canada

Received September 6, 2000; Revised Manuscript Received January 19, 2001

ABSTRACT: We extend our lattice model of gel electrophoresis (and diffusion) to the study of the continuum limit (no lattice effect) for hard spherical particles migrating in periodic and random three-dimensional gels. To reach the continuum limit, the mesh size of the system is progressively decreased until a clear extrapolation to the continuum limit (where the size of the lattice parameter is infinitely small in comparison to the size of the gel fibers) can be done. Various types of gel are studied, starting from simple periodic parallel and straight fibers to a representation of a more realistic gel formed of irregular, cross-linked fibers placed along random directions. Our mobility data for pseudospherical particles in the continuum limit are interpreted in terms of the obstruction model of diffusion.

I. Introduction

Over the past few years we have developed a new microscopic model to study the gel electrophoresis (or, equivalently, the thermal diffusion) of hard particles. Our lattice model allows us to compute exact reduced mobilities μ^* (or exact reduced diffusion coefficients D^*) as well as exact free available volumes, f, for arbitrary gel structures and particle shapes in any dimension $d \geq 2$.[1−6] Because of the large computer resources needed to obtain exact results, we were first forced to study relatively simple and somewhat unrealistic particles and gels (e.g., two-dimensional systems, square particles, etc.). However, we recently proposed a much more efficient numerical approach[7,8] that makes it possible to tackle much larger (hence more realistic) analyte−gel systems. This article is the first one in which we study pseudospherical analytes migrating in realistic three-dimensional gels. Such systems closely correspond to the main reason why Ogston models are used to interpret electrophoretic data.[1−13]

Originally, the main goal of our investigation was to verify the standard Ogston−Morris−Rodbard−Chrambach (OMRC) model,[9−11] as well as a data analysis method based mostly on the so-called Ferguson plot.[12,13] In the framework of the OMRC model, the low-field reduced mobility $\mu^*(C)$ of an analyte is assumed to be equal to its free available volume $f(C)$:

$$\mu^*(C) = \frac{\mu(C)}{\mu_0} = f(C) = 1 - \phi(C) \tag{1}$$

where μ_0 is the free (no obstacle) mobility, $\phi(C)$ the excluded volume, and C the obstacle concentration. While never proven (experimentally or theoretically),[14] this assumption is the starting point the OMRC model, which is widely used within the electrophoresis community.

For a specific system, namely a spherical particle in a random array of infinitely long (but un-cross-linked) fibers, Ogston[9] showed that the fractional volume available to the analyte was given by

$$f(C) = \mathrm{e}^{-\pi(R+r)^2/4a^2} \tag{2}$$

where R, r, and $a(C)$ are the radii of the analyte, gel fiber, and gel pore, respectively. For the Ogston ideal "gel", the mean pore size $a(C)$ is given by (this formula was derived for infinitely thin fibers)

$$a(C) = \frac{1}{\sqrt{4\nu l}} \propto \frac{1}{\sqrt{C}} \tag{3}$$

where ν is the concentration of fibers per unit volume and l the average fiber length. This leads to

$$\mu^*(C) = f(C) = \mathrm{e}^{-KC} \tag{4}$$

where $K \propto (R + r)^2$ is the so-called retardation coefficient. This implies that the Ferguson plot ($\ln \mu$ vs C or $\ln \mu^*$ vs C) should be linear. In such cases, one can easily extract the retardation coefficient from the slope. Furthermore, when the square root of the retardation coefficient is plotted as a function of the particle radius R, the value of R where $K(R) = 0$ (found by extrapolating $K^{1/2}$ to negative values of R) gives $-r_K$, which is an estimate of the fiber radius r.

An effective mean pore size a_K can also be estimated when using the OMRC model to analyze experimental data. For example, the plot of the root of the log of the mobility as a function of the particle size ($\sqrt{-\ln\mu}$ vs R) should yield a straight line with a slope given by the inverse of the pore size. More frequently, one assumes that $R \gg r$ to obtain a value from the data using the fact that we then have $\mu^*(R=a) = \mathrm{e}^{-\pi/4} \simeq {}^1/_2$.[15]

In the previous parts of this series, we studied square or cubic particles diffusing in two-dimensional periodic, random, and fuzzy gels (parts I, II, III, and V[1−3,5]) and three types of three-dimensional periodic gels (parts IV and V[4,5]). For all these sieving gels, the basic assumption of the OMRC model, namely, that the low-field gel electrophoresis mobility μ of a (rigid) particle is proportional to the fractional gel volume $f = 1 - \phi$ available to the particle, was found to be inaccurate, except for the nonrealistic case where the gel constraints (the obstacles) were reset randomly at each time step (corresponding to a mean-field approximation or an annealed gel).[1] We also showed that, for two-dimensional

* To whom correspondence should be sent. E-mail: gslater@science.uottawa.ca.

10.1021/ma001544o CCC: $20.00
Published on Web 04/06/2001

gels, the curvature of the so-called Ferguson plot was related to the degree of disorder in the gel[1] and that certain gel architectures can have nontrivial sieving properties.[3] We further demonstrated that a modified Ferguson plot can nevertheless provide useful semiquantitative information about the gel properties (such as a reliable estimate of the mean pore size)[1−3] and that the occasional presence of inflection points in the Ferguson plot may be explained by the effect of obstacle−analyte attractive interactions.[5] Finally, we studied the mobility of small oligomers and found the Ogston model to be insufficient to describe the movement of these molecules.[6]

In this article, we present a detailed study of pseudospherical analytes migrating in three-dimensional gels, clearly a very Ogston-like system.[9] Our aim is to study the continuum limit and to draw fundamental conclusions about realistic systems without hydrodynamic interactions. The paper is organized as follows. After a short overview of our model and numerical techniques (section II), the mobility of the analyte is calculated for infinite periodic straight fibers placed perpendicularly to the net motion of the particle (section III). In section IV, the mobility is calculated for four types of three-dimensional gels. The first two are periodic and are made of straight infinite fibers placed along the three orthogonal axes with and without cross-links (section IV). The last two are random: one is made of straight orthogonal fibers places randomly, while the last one is made of irregular cross-linked fibers placed along random directions. Our conclusions are presented in section V.

II. The Model

Many computational methods can be used to study the diffusion (random or biased, with or without constraints) of a particle. However, most of them, like molecular dynamics and Brownian dynamics simulations, are very CPU intensive, and the steady-state regime is sometimes hard to reach. To obtain better statistics faster, lattice models can be used. In such models the migration of the particle is represented by a random walk on a finite-size lattice (usually with periodic boundary conditions) where certain sites are forbidden (this may represent, e.g., gel fibers). These investigations often involve Monte Carlo methods and, with modern computers, allows one to follow the diffusion of millions of independent (or even interacting) particles over physically meaningful distances. The approach is quite simple. One simply records the position x of the analyte as a function of time t and then estimates the mobility:

$$\mu = \frac{1}{\epsilon} \lim_{t\to\infty} \frac{\langle x(t)\rangle}{t} \tag{5}$$

where ϵ is the dimensionless field intensity. In absence of a field one can estimate the diffusion coefficient as

$$D = \lim_{t\to\infty} \frac{\langle x(t)^2\rangle}{2t} \tag{6}$$

Lattice Monte Carlo simulations can also provide information about the short time dynamics of the particles. However, when only the low-field steady-state regime (D of μ) of an isolated particle is of interest, we demonstrated in part I of this series that lattice simulations are not necessary since the Monte Carlo algorithm can in fact be solved exactly for the mobility (or for the diffusion coefficient) in the zero-field limit.[1,7] In other words, we find directly μ or D without recording x as a function of time. This greatly simplifies the analysis since we then obtain exact values. However, our method is only useful for isolated analytes in the zero-field limit.

A. The Lattice Random-Walk Model. In the lattice random-walk model, the particle moves by making discrete jumps of length $L = 1$ (the lattice parameter) and duration $\tau = 1$ (in scaled units). For a rigid particle (which can be of any desired shape; note however that particle rotation is not allowed) evolving on a three-dimensional cubic lattice with an electric field ϵ pointing in the $+x$ direction, the probabilities for the next jump to be in the various possible directions ($\pm x$, $\pm y$, and $\pm z$) are, to first order in ϵ, given by[1]

$$p_{\pm x} = \frac{1 \pm \epsilon}{6} + O(\epsilon^2), \quad p_{\pm y} = p_{\pm z} = \frac{1}{6} \tag{7}$$

The rules for this model are quite simple: at each time step the particle moves to one of the six adjacent sites according to the probabilities given by eq 7. However, since a particle cannot overlap with an obstacle (representing a gel fiber), a jump leading to this situation is rejected and the particle returns to its previous position. Note that the current time is increased by the time step ($\tau = 1$) even when the jump is rejected. The jump rejection rule models the steric (hard core) interactions between the analyte and the gel fibers. Other types of analyte−fiber interactions are not taken into account but can also be included.[5]

B. Exact Mobilities. The mobility μ is defined as the velocity v of the particle divided by the intensity ϵ of the applied field (eq 5). Consider a particle of mass M (where M is the number of lattice cells occupied by the particle) evolving on a lattice of size $s \times s \times s$ (using periodic boundary conditions). We first calculate the steady-state probability of presence (n_i) of the particle on each of the available sites (defined as the sites where the center of mass of the particle can be placed without having any part of the particle overlapping with gel fibers). Since the probabilities n_i are coupled to each other (because of the jump dynamics), the problem can be reduced to the solution of a large system of linear equations. We then calculate the mean local velocity of the particle on each site (v_i). This step is straightforward since the latter depends only on the occupancy (by an obstacle) of the nearest-neighbor sites.[1] The average velocity of the particle is then given by $v = \sum_i n_i v_i$. The reader can consult parts I−V of this series[1−5] as well as refs 7 and 8 for more details.

Since we are interested in the low-field limit $\epsilon \to 0$, all our calculations are carried to first order in ϵ, and we drop all higher order terms. Recently, we found that we can actually eliminate the need for an arbitrary (finite) value of ϵ in the case of a vanishing electrical field.[7,8] The calculation of the exact mobility is then reduced to the solution of a purely numerical (no reference to the field parameter ϵ) system of S linear equations (where $S \le s^3$ is the number of available sites) of the form (we use the Dirac notation where matrices are represented by uppercase letters, scalars by lowercase letters, and row and column vectors by respectively bras and kets):

$$A_I|n_\epsilon\rangle = -A_\epsilon|n_I\rangle \tag{8}$$

where A_I, A_ϵ, $|n_I\rangle$, and $|n_\epsilon\rangle$ are the field-independent (subscripts I) and field-related (subscripts ϵ) terms of the transition matrix $A = A_I + \epsilon A_\epsilon$ and probability vector $|n\rangle = |n_I\rangle + \epsilon|n_\epsilon\rangle$. Note that the only unknown here is the probability correction term $|n_\epsilon\rangle$. Therefore, with our approach, the problem of finding the zero-field mobility of an analyte is reduced to the solution of a (large) system of linear equations. This system of linear equations can be directly solved using, e.g., Maple or Mathematica, in which case the mobility can be expressed in terms of a (huge) rational fraction or with a number of well-known numerical algorithms integrated within a lower level language (e.g., Fortran, C) program. With our homemade Fortran program (which automatically writes and solves the linear equations), we have been able to solve problems corresponding to lattices as large as 80 × 80 × 80 on standard Pentium-based workstations. Once $|n_\epsilon\rangle$ is found, the resulting scaled mobility can easily be computed as

$$\mu^* = \frac{v}{\mu_0 \epsilon} = \frac{\langle v|n\rangle}{\mu_0 \epsilon} = \frac{\langle v_1|n_\epsilon\rangle + \langle v_\epsilon|n_I\rangle}{\mu_0} \tag{9}$$

where μ_0 is the free (no obstacle) mobility of the particle. We refer the reader to refs 7 and 8 for a complete derivation of the preceding equations.

C. Diffusion Problems. It turns out that our approach can also be used to study diffusion problems since the zero-field mobility is related to the diffusion coefficient through the Nernst−Einstein relation:

$$D^* = \frac{D}{D_0} = \lim_{\epsilon \to 0} \frac{\mu}{\mu_0} \tag{10}$$

where D and D_0 are respectively the diffusion coefficients of the analyte with and without obstacles. Therefore, it is possible to reinterpret all the data in the current article as being related to the diffusion of spherical particles in quenched gels when the hydrodynamic interactions are neglected. Obstructed diffusion is of great interest in a large number of physical, biological, and chemical problems.[16−20] Numerous groups have studied this problem, and an impressive number of analytical and empirical theories, often contradicting one another, have been developed. Amsden recently reviewed different models and concluded that the obstruction models in general provided the best agreement to the experimental data for heterogeneous hydrogels.[17] But even when only steric interactions are considered, many competing theories still remain. Apart from the standard Ogston model, one of the most often used is probably the stretched exponential:[21]

$$D^* = \mathrm{e}^{-a\phi^b} \tag{11}$$

where both a and b are constants. In his review, Amsden concluded that for heterogeneous gels the stretched exponential and the very simple Tsai and Streider model[18]

$$D^* = \frac{1}{1 + \frac{2}{3}\phi} \tag{12}$$

were the most consistent with the literature data.

Finally, the diffusion problem can also be related to other transport properties. For example, many groups have studied the electrical properties (i.e., the conductivity) of a conductor containing nonconducting patches (e.g., holes) using the diffusion algorithm.[19]

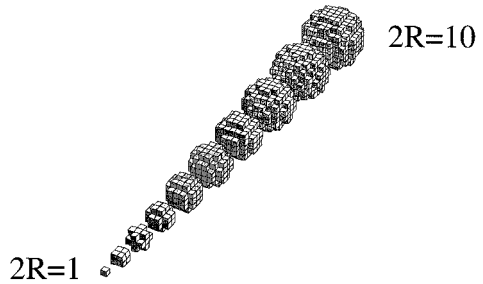

Figure 1. Spherical particles (on a cubic lattice) for diameters $2R$ varying from 1 to 10.

D. Random Systems. Our method allows one to obtain the exact mobility of the analyte for any specific finite size lattice system (using periodic boundary conditions) of any dimensionality ($d \geq 2$). For periodic systems of obstacles, this means that one can obtain the exact mobility in one iteration. However, the situation is different if there is any degree of randomness in the obstacle distribution. Using our approach, it is possible to find the exact mobility for specific realizations of the disorder, but we then need to average over various realizations to yield a meaningful mobility $\mu^*(C)$ or diffusion coefficient $D^*(C)$. This introduces a statistical error and explains why an uncertainty will be associated with the mobilities for the random systems. We also need to be careful with finite size effects. When calculating an average mobility for a disordered system, we are usually interested in the thermodynamic limit (an infinite system, $s \to \infty$). To obtain reliable results, the system has to be sufficiently large so that finite-size effects are negligible in comparison with the uncertainty resulting from the ensemble averaging process. For a complete discussion on these topics, see ref 8.

E. Modeling Spheres on a Cubic Lattice. For our system to be the most realistic possible, we chose to give the diffusing particle a "spherical" shape (and the gel fibers a "cylindrical" shape). Since the particles are evolving on a cubic lattice, our "spheres" are rather peculiar. Figure 1 shows the shape of our spherical particles (on a cubic lattice) for diameters $2R$ varying from 1 to 10. To build a pseudospherical analyte of size $2R$, we first center the particle (at the center of a unit cube for odd diameters and on a lattice site for even diameters) and we add the unit cubes whose centers are within a distance R of the starting position. The particles obviously become perfect spheres in the $R \to \infty$ limit.

Note that, for the calculation of the mobility, the problem of a particle of radius R diffusing in a gel with cylindrical fibers of radius r is equivalent to the problem of a particle with an effective size $r' = r + R$ diffusing in a gel with infinitely thin fibers (or vice versa). The relevant parameter of the problem is thus the excluded volume $\phi(R,r,C)$, which corresponds to the fraction of the volume not accessible to the analyte when the latter is reduced to a pointlike object. When calculating the mobility, we will use the simple procedure[22] of replacing a given system by a pointlike analyte and gel fibers of effective size $r' = r + R$. To obtain the results in term of "real" system parameters (R, r, and C), the relation between the excluded volume ϕ, the particle size R, the gel fiber size r, and the gel concentration C needs to be found. This relation can be very simple for periodic

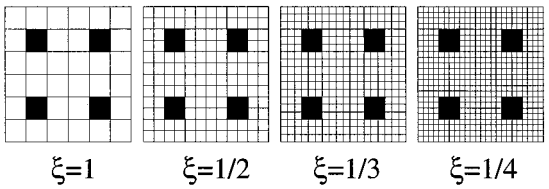

Figure 2. Transformation of a simple lattice problem as the mesh size ξ is decreased. The "gel" is made of isolated square obstacles placed periodically; the concentration C (or volume fraction ϕ) is $^1/_9$.

structures but can become quite complicated when considering complex gels. The original Ogston paper gives an example of such a calculation,[9] but real gels are different because they are cross-linked.

Note that it is not clear what a pointlike object corresponds to on a lattice. For instance, on a two-dimensional square lattice, a lattice site can be seen either as a pointlike object (i.e., a lattice point vertex) or as a 1×1 plaquette. While important for small analytes and fibers, this distinction becomes irrelevant in the continuum limit. In the following we will consider that the migrating analyte is a pointlike object (a lattice point vertex) and that the excluded volume ϕ is the fraction of lattice sites inaccessible to the analyte.

F. The Continuum Limit. The mobility (or diffusion coefficient) generally depends on the type of lattice used. This is so because the lattice amplifies the effect of the particle and obstacle shapes and modifies the correlation between consecutive events. To obtain experimentally relevant results, we need to consider the continuum limit, i.e., the limit where the size of the lattice parameter is infinitely small in comparison with the size of the analyte and obstacles. In this limit, the results are independent of the lattice type and correspond to the ones obtained with off-lattice Monte Carlo simulations. These two conditions are met, and our method thus provides valid and very precise numerical data with much less computing time.

In a separate article, we discuss a simple method to reach the continuum limit.[23] The procedure is to progressively decrease the "mesh size" ξ of a given problem, i.e., to decrease the relative size of the lattice parameter while keeping R and r constant. For example, let us consider the problem shown in Figure 2. In this system, a pointlike particle is migrating through a two-dimensional gel made of isolated square obstacles placed periodically. The separation between the obstacles is set to twice their linear size, resulting in a gel concentration (volume fraction) $\phi = C = {}^1/_9$. With the effective radius set at $r' = {}^1/_2$, the mesh size ξ is then reduced to zero. Figure 2 shows different views of the gel system for decreasing ξ while Figure 3 shows the resulting reduced mobility μ^* as a function of ξ for a pointlike analyte. The mobility converges toward $\mu^* = 0.922(1)$ in the $\xi \rightarrow 0$ (continuum) limit.

To obtain the dependence of the mobility upon the excluded volume ϕ (or the obstacle concentration C), one needs to repeat the procedure for different values of excluded volumes ϕ and then fit the ($\xi \rightarrow 0$) extrapolated mobility data. Because we did not have any specific mathematical formula to use to fit our numerical data, we chose to use the general polynomial form

$$\mu^*(\phi) = 1 + \sum a_i \phi^i \tag{13}$$

Since we are mainly interested in the low concentration limit $\phi \ll 1$, only the first few coefficients are relevant. To obtain the a_i coefficients with more accuracy, we actually fit the function

$$g = \frac{\mu^*(\xi,\phi) - 1}{\phi} \tag{14}$$

In this case, a_1 correspond to the ordinate axis, a_2 to the slope, and a_3 the curvature of the plot. This also ensures that the expansion in integer powers of ϕ is valid. For example, if there were a $\phi^{1/2}$ term in the $\mu(\phi)$ expression, the g function would actually diverge at $\phi = 0$.

Another approach to reach the continuum limit consists of finding the dependence (also in a polynomial form) of the mobility $\mu^*(\xi,\phi)$ upon the excluded volume ϕ for a large number of mesh sizes ξ and then estimate the resulting polynomial coefficients $a_i(\xi)$ in the $\xi \rightarrow 0$ limit. While less intuitive, this latter approach gives better results for small excluded volumes. For the Ogston hypothesis to be correct (eq 1), we must have $a_1 = -1$ and $a_{i\geq 2} = 0$.

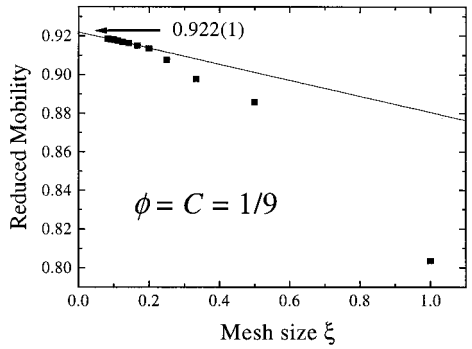

Figure 3. Mobility of a pointlike analyte as a function of the mesh size ξ for the system shown in Figure 2.

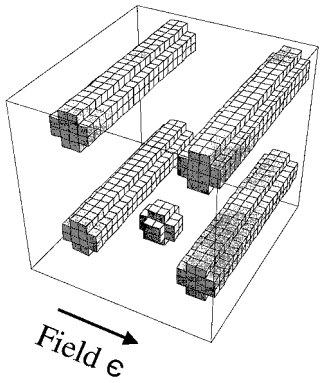

Figure 4. A three-dimensional periodic gel made of straight, parallel, and infinitely long fibers of radius $r = {}^1/_4$. There is no fiber aligned in the field direction. An analyte of radius $R = {}^1/_4$ is also shown. The mesh size is $\xi = {}^1/_8$.

III. Straight Fibers Perpendicular to the Field

Figure 4 shows a particle migrating in a "gel" made of straight, infinitely long parallel fibers. While the system is not a good representation of a gel, its symmetry of translation (the fibers are placed periodically) allows us to reduce it to the periodic two-dimensional system shown in Figure 5a. (We limit our study to the migration perpendicular to the gel fibers.) Since two-dimensional systems are computationally much easier to study than three-dimensional ones, this special case is a useful starting point for our investigation.

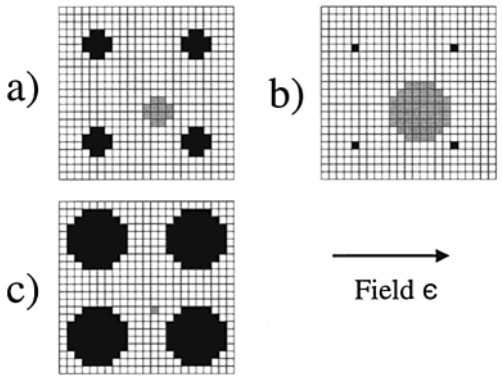

Figure 5. (a) Two-dimensional representation of the system shown in Figure 4. This problem is equivalent to that of a particle with an effective size $R' = r + R = 1/2$ diffusing in a gel with infinitely small fibers (b) or to the one of a pointlike particle and gel fibers of effective size $r' = r + R = 1/2$ (c). Note that, for visual reasons, the pointlike objects are shown as 1 × 1 plaquettes. The mesh size is $\xi = 1/8$.

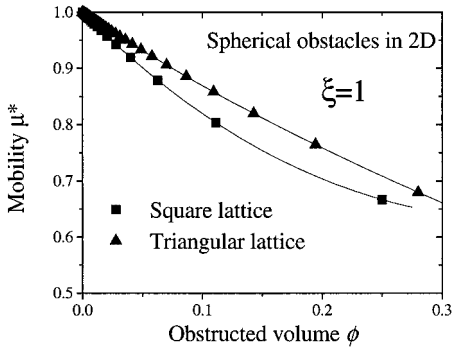

Figure 6. Mobility μ^* as a function of the excluded volume ϕ for a system made of two-dimensional periodic obstacles, using a square and a triangular lattice (in both cases the mesh size is $\xi = 1$). The solid lines are the best third-order polynomial fits.

A. Obtaining the Mobility. As briefly discussed in section IIE, when one is only interested in the mobility, the system shown in Figure 5a is formally equivalent to those of Figure 5b,c. Note that because of the imperfections of our lattice spheres, this equivalence will only be exact in the continuum limit ($\xi \to 0$).

We will now focus on finding the dependence of the mobility of a pointlike analyte upon the excluded volume ϕ (in terms of a polynomial form) for different mesh sizes (ξ). The procedure is the following. First, a mesh size ξ is chosen. Then the zero-field mobility of the particle is calculated exactly, using the method described in section IIB and refs 7 and 8, for increasing separations between the gel fibers (i.e., for decreasing excluded volume fractions ϕ). The excluded volume ϕ corresponds to the proportion of sites occupied by the effective fibers. Finally, a polynomial fit of the form

$$\mu^*(\xi,\phi) = 1 + \sum a_i(\xi)\phi^i \qquad (15)$$

is used to describe the dependence of the mobility upon the excluded volume ϕ. Figure 7 shows an example of such fit for a system with a lattice parameter $\xi = 1$, using a triangular and a square lattice. As expected, the two lattices give different results except in the trivial case $\phi = 0$. For all excluded volumes ϕ, the analyte has a larger mobility on the triangular lattice because of the larger lattice coordination number; i.e., the analyte has more ways to avoid consecutive collisions with an obstacle. In both cases, the curvature is positive, a characteristic of periodic gels.

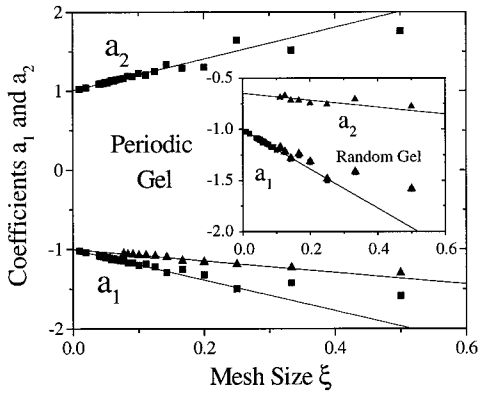

Figure 7. Coefficients $a_1(\xi)$ and $a_2(\xi)$ vs the mesh size ξ for a system made of two-dimensional periodic obstacles. The extrapolated values are $a_1(0) = -1.003(6)$ and $a_2(0) = +1.01(5)$ for the square lattice and $a_1(0) = -1.00(1)$ for the triangular lattice Inset: coefficients $a_1(\xi)$ and $a_2(\xi)$ for 2D isolated obstacles placed randomly, along with the a_1 data for the periodic obstacles (both results correspond to cases with a square lattice).

B. The Continuum Limit. The procedure described in section IIIA has been carried out for mesh sizes ξ varying from 1/100 to 1 on square and triangular lattices. Figure 7 shows the first coefficient a_1 for square and triangular lattices as a function of the mesh size ξ. The fluctuations of these very precise values can be explained by the roughness of our lattice "spheres" (our gel fibers will only take the perfect cylindrical shape in the $\xi \to 0$ limit). As expected, the results for the first coefficient is independent of the lattice type in the continuum limit, and the results converge toward the same value ($a_1(\xi \to 0) = -1.002(8)$) for both lattices. Similarly, we obtain $a_2 = +1.01(5)$ for the square lattice (although less precise, the results for the triangular lattice agree with this value; not shown). In fact, the extrapolated value for the third coefficient a_3 (not shown) also converges toward a value of -1 (however, the uncertainties are much larger). These results seem to indicate that an excellent description of the dependence of the mobility upon the obstructed volume (for small values of ϕ) is provided by the simple formula

$$\mu^*(\phi) = \frac{1}{1+\phi} \simeq 1 - \phi + \phi^2 - \phi^3 + \ldots \qquad (16)$$

This can be verified in Figure 8 where the inverse of the mobility is plotted as a function of the excluded volume for various mesh sizes ξ. Simple linear relations provide excellent agreement with the data, especially for small mesh sizes, for excluded volumes as large as $\phi \cong 20\%$. Furthermore, the data become closer to the relation given by eq 16 as the mesh size ξ decreases, indicating that it is indeed the correct relation in the continuum limit. This result, which has been predicted theoretically in ref 18 using variational principles, agrees with the OMRC model ($\mu = 1 - \phi$) to first order. Of course, this formula is not valid for large values of ϕ since it does not predict a percolation threshold. (For instance, eq 16 predicts $\mu = 1/2$ at $\phi = 1$, while we must have $\mu = 0$ when $\phi \geq \pi/4$ for our system of cylindrical fibers.) Nevertheless, it would give essentially perfect fits for all realistic "gel concentrations" (e.g., $\phi < 20\%$) in the continuum limit. In a separate article,[23] we showed that near the percolation threshold $\phi = \phi^* =$

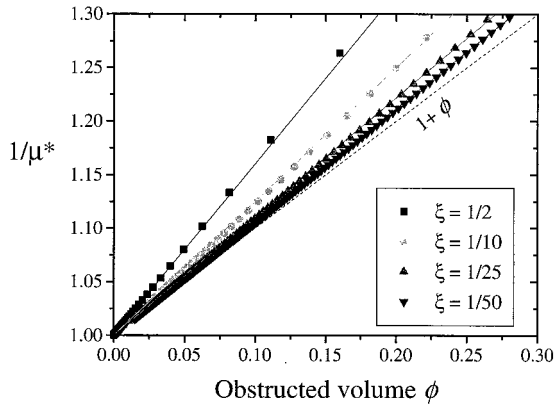

Figure 8. Inverse mobility $1/\mu^*$ vs the obstructed volume ϕ for various mesh sizes ξ. The solid lines are linear fits, and the dashed line is eq 16, the suggested asymptotic result for the $\xi \rightarrow 0$ continuum limit.

$\pi/4$ the data agree with a power-law decay, and we proposed a simple interpolation function which gives excellent agreement with our data for all values of the obstructed volume ϕ. We also showed that eq 16 can be generalized to the case of "hyperspherical" periodic obstacles in d dimensions:

$$\mu^*(\phi) = \frac{1}{1 + \frac{1}{1+d}\phi} \tag{17}$$

for low values of excluded volume.

C. Randomly Placed Fibers. In a previous part of this series,[1] we reported that adding randomness in the distribution of obstacles does not affect the first coefficient (a_1) but does change the second one (a_2). In fact, we showed that, in the case of isolated square obstacles in two dimensions, the sign of the second coefficient actually changes from positive to negative as the degree of randomness is increased. However, all our calculations were done using a single mesh size $\xi = 1$. To verify that this effect is still present in the continuum limit, we repeated the calculations for various mesh sizes. The inset of Figure 7 shows the first two coefficients as a function of the mesh size for a two-dimensional gel made of randomly placed circular obstacles (or, equivalently, for the system shown in Figure 4 but with randomly distributed parallel fibers). The data for the first coefficient (a_1) of the periodic gel shown in Figure 4 were also added to the plot. As expected, the randomness does not affect the first coefficient, and the two sets of data coincide perfectly. However, the second coefficient converges to a negative value: $a_2(\xi \rightarrow 0) = -0.66(2)$. Thus, the effect previously observed was real; i.e., it was not a lattice artifact: randomness does change the sign of the second coefficient a_2.

D. Ferguson Plots and Gel Parameters. Following our previous work,[2−4] we now analyze our data in terms of the standard OMRC model. First let us define the effective retardation coefficient as

$$K(R) = -\lim_{C \rightarrow 0} \frac{\partial \mu^*(C)}{\partial C} \tag{18}$$

For this system of parallel straight fibers, the excluded volume of the analyte is given exactly by

$$\phi(C) = \frac{(R+r)^2}{r^2} C \tag{19}$$

Substituting this relation into eq 13, we obtain

$$\mu^* = 1 + \sum a_i(r') \frac{(R+r)^{2i}}{r^{2i}} C^i \tag{20}$$

In the continuum limit we have $a_1(\xi \rightarrow 0) = -1$; thus

$$K(R) = -\lim_{C \rightarrow 0} \frac{\partial \mu^*(C)}{\partial C} = \frac{(R+r)^2}{r^2} \tag{21}$$

According to these results, finding the value of the fiber size by extrapolating $K^{1/2}$ to negative values of R until $K^{1/2} = 0$ is thus perfectly valid as long as the fiber concentration is kept small.

For this simple gel, the concentration is given by

$$C = \frac{\pi r^2}{(2a(C) + 2r)^2} \tag{22}$$

where $2a(C)$, the pore diameter, is trivially given by the separation between two consecutive obstacles. (This is the size of the largest particle that would have a nonzero mobility in this system.) For small concentrations ($a(C) \gg r$), we thus have $a(C) \propto 1/\sqrt{C}$, which is consistent with the OMRC theory and Ogston's calculation.[9] Substituting this result into eq 20, we get

$$\mu^* = 1 - \frac{\pi(R+r)^2}{4a^2} + \ldots \simeq e^{-\pi(R+r)^2/4a^2} \tag{23}$$

which is the main result of the OMRC model (eq 2) although our definition of the retardation factor K slightly differs from that given in eq 4. Therefore, although OMRC's fundamental assumption eq 1 is invalid, the data analysis procedure based on this model remains useful in practice.

IV. Three-Dimensional Gels

We now look at more realistic three-dimensional systems where the fibers are not restricted to point in only one direction. A prediction for the dependence of the mobility upon the excluded volume can be made using a simple argument. The previous section demonstrated that when the gel fibers are placed perpendicularly to the movement of the particle, the mobility of the particle can be expressed as (at least for realistic gel concentrations)

$$\mu^* = \frac{1}{1 + \phi(C)} \tag{24}$$

Since fibers parallel to the motion of the particle will not affect its net migration, we can argue that the reduced mobility of the analyte should be (at least as a first approximation) given by

$$\mu^* = \frac{1}{1 + \frac{2}{3}\phi(C)} \tag{25}$$

when $^1/_3$ of the gel fibers are parallel to the motion. Note that this relation is equivalent to the Tsai and Streider equation (12).

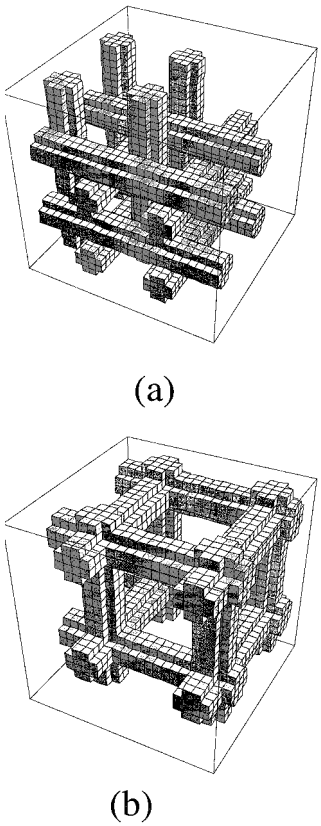

Figure 9. Two periodic three-dimensional gels with straight orthogonal fibers. (a) Without cross-link. (b) The gel forms a cross-linked network with a cagelike structure.

A. Periodic Gels. Figure 9 shows two periodic gels formed of straight fibers placed along the three orthogonal axis. In the first case (Figure 9a), each fiber follows an axis placed at the center of two other orthogonal fibers. Therefore, this gel is not cross-linked. In the second case (Figure 9b), three orthogonal fibers share one or more sites (depending on the size of the fibers) so that the gel forms a network with a cagelike structure.

As in section III, the dependence of the mobility upon the excluded volume ϕ was calculated in terms of a polynomial for decreasing mesh sizes ξ. As expected, the first coefficient (a_1) of the polynomial expression (eq 13) is identical for the two gels. In the low excluded volume limit the number of cross-links is very small and does not affect the migration of the analyte. The results for a_1 for the gel without cross-links (Figure 9a) are shown in Figure 10 as a function of ξ. The data for the gel with cross-links (Figure 9b) agree with Figure 10 (not shown). Again, the small fluctuations are due to the imperfect lattice "spheres". The extrapolation to the continuum limit ($a_1(\xi \rightarrow 0)$) is remarkably close to the predicted value of $-2/3$. For larger values of excluded volume ϕ, the specific geometry of the gel is important: this is why the two gels have different coefficients a_i for $i > 1$. This can be seen in the inset of Figure 10 where the extrapolated mobility $\mu^*(\xi \rightarrow 0)$ is plotted as a function of the total obstructed volume ϕ. While the mobility for the gel without cross-links (Figure 9a) follows nicely eq 25 for obstructed values as large as 10%, the mobility for the cross-linked gel (Figure 9b) diverges from eq 25 for relatively small obstructed volumes (~5%). In fact, for the latter gel, the sign of the second coefficient a_2 is different from the one predicted by eq 25! We thus see

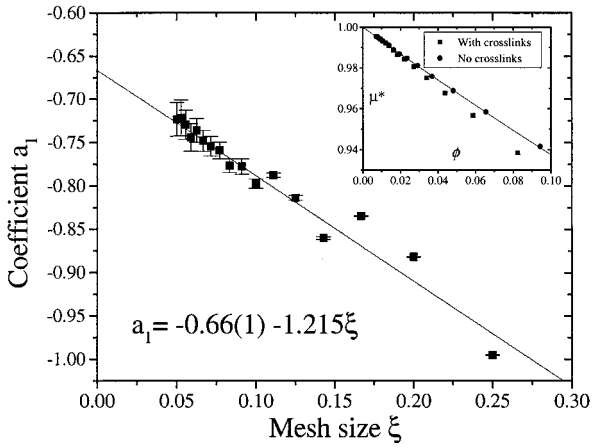

Figure 10. First coefficient of the polynomial expression of the dependence of the mobility upon the excluded volume for the gel shown in Figure 9a. The $\xi \rightarrow 0$ extrapolated value is $a_1 = -0.66(1)$. Inset: reduced mobility μ^* vs the total obstructed volume ϕ for the gels shown in Figure 9. The line is eq 25.

that the structure of the gel has an important effect on the dependence of the mobility upon the excluded volume. Therefore, a general relation describing the dependence of the mobility upon the excluded volume ϕ, independent of the gel structure, can only give rough estimates. This is a clear demonstration of the failure of the OMRC hypothesis (eq 1). This also shows that eq 25 is not general but corresponds to the precise gel shown in Figure 9a.

B. Random Gels. Although instructive, all the cases studied until now (2D systems, periodic systems, straight fibers, etc.) were probably poor representations of gel electrophoresis. We now look at the case of two different random gels. In the first one, the gel fibers are placed randomly in space but kept straight and parallel to the *x*, *y*, and *z* axes. This type of un-cross-linked gel is very close to the one originally proposed by Ogston.[9] Figure 11a shows an example of such a system.

The second one is the most realistic one since it is formed of irregular cross-linked fibers placed along random directions (Figure 11b). To generate such a gel, we first join two sites, randomly chosen, by a biased random walk. During this random walk, the "jumping" probability (along one of the orthogonal axis) is simply given by the ratio of the number of sites separating the two ends along this direction to the total separation. After completion of the first fiber, we choose two occupied sites (already part of the gel) and join them using the same rules but forcing them to go out of the primitive cell via the periodic boundary conditions (PBC). This last step is repeated until the right concentration (previously chosen) is obtained. We finally increase the fibers size by a factor r'/ξ in order to obtain the right mesh size. This leads to a connected network of "cylindrical" fibers with somewhat random shapes but still fairly rigid. While this gel still suffers from many imperfections, it is clearly the most realistic representation of a true gel that we have studied.

As we did for the other gels, we plot the coefficient a_1, which characterizes the low-concentration limit, as a function of the mesh size ξ (Figure 12). For comparison, the data for the non-cross-linked periodic gel described in the previous section were added to the plot. We note that, for both random gels, the values of the a_1 coefficient are apparently identical to the ones obtained

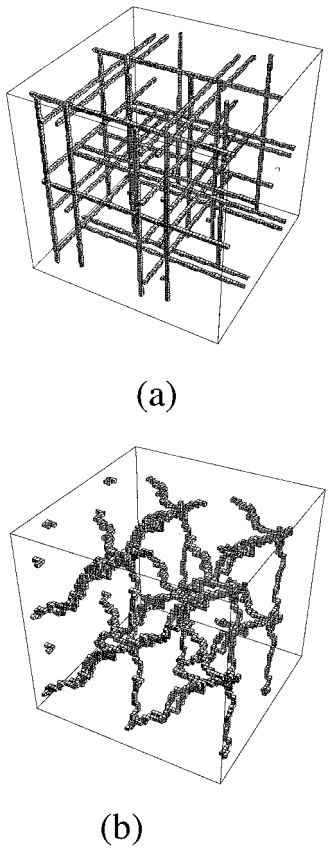

Figure 11. Two types of random three-dimensional gels. (a) Straight fibers placed randomly along the three orthogonal axis. (b) Gel formed of irregular, cross-linked fibers placed along random directions. In both cases, the primitive cell (of periodicity $s = 30$) is repeated eight times for a better view.

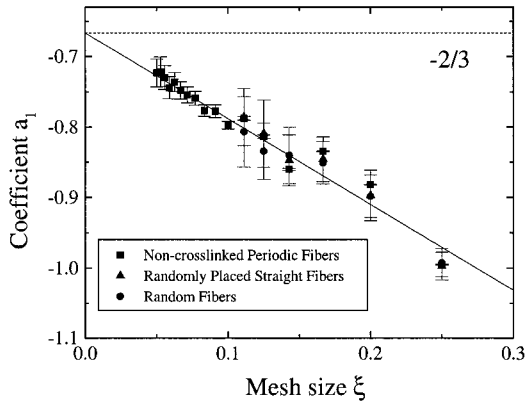

Figure 12. First coefficient (a_1) of the polynomial expression of the dependence of the mobility (μ^*) upon the excluded volume ϕ for the gels shown in Figure 11. The data for the periodic gel (Figure 9) are added for comparison. All extrapolated values are consistent with the predicted value of $-2/3$.

for the periodic gel, thus leading to an expected extrapolated value of $-2/3$. This confirms our previous results that the first coefficient changes with the shape of the obstacles but is independent of the distribution of the obstacles. Therefore, we expect to have $a_1 = 2/3$ for all representations of long stiff fibers, as long as the distribution of the fibers is isotropic. The higher coefficients ($a_{i\geq 2}$), however, are not universal and are strongly affected by the specific geometry of the gel.

C. Gel Parameters. Following section IIID, we now analyze the data using the method suggested by the OMRC model. For our first system (the non-cross-linked periodic gel shown in Figure 9a), the excluded volume is simply given by

$$\phi(C) = \frac{(R + r)^2}{r^2} C \tag{26}$$

leading to (using the fact that we have $a_1 = -2/3$)

$$K(R) = -\lim_{C\to 0} \frac{\partial \mu^*(C)}{\partial C} = \frac{2(R + r)^2}{3r^2} \tag{27}$$

For the other gels (Figures 9b and 11a,b), the presence of cross-links will slightly change the dependence $\phi(C)$ of the excluded volume upon the concentration. For low concentrations, however, eq 26 is a very good approximation. Therefore, the plot of the square root of the retardation coefficient K as a function of the particle radius R will lead to a straight line, and again the value of R at which $K(R) = 0$ will give the fiber radius r.

In the case of the non-cross-linked periodic gel (Figure 9a), the obstacle concentration can be expressed as

$$C \simeq \frac{3\pi r^2}{(2a(C) + 2r)^2} \tag{28}$$

For low concentrations ($a(C) \gg r$) we thus find $a(C) \propto 1/\sqrt{C}$, which is again consistent with the OMRC theory. Finally, substituting eq 2 into the polynomial fit, we get

$$\mu^* \simeq 1 - \frac{2\pi(R + r)^2}{4a^2} + \ldots \tag{29}$$

Again, we find a form very similar to the one used with the OMRC model (eq 2), although new numerical coefficients have appeared.

V. Conclusions

In this article we presented a study of pseudospherical analytes migrating in three-dimensional gels without hydrodynamic interactions. We showed that the use of a lattice to treat diffusion processes has an important impact on the numerical results. For example, the dependence of the mobility (or the diffusion coefficient since $\mu^* = D^*$ in the low-field limit) upon the excluded volume of the analyte changes drastically if we vary the mesh size of a given problem or if we change the lattice type (e.g., square vs triangular lattice). However, if one properly extrapolates toward the continuum limit, where the lattice parameter is infinitely small in comparison to all the other length scales, the results become independent of the lattice type and correspond to those of similar off-lattice simulations (but they require less CPU time). Our study of the continuum limit revealed that the geometry of the gel has a strong impact on the dependence of the mobility upon the excluded volume, thus confirming our previous work. If we express our results in terms of a polynomial expansion, we found that the first coefficient, which characterizes the low excluded volume limit, changes with the shape of the obstacles but is independent of the distribution of the obstacles. For example, we found $a_1 = -1$ for isolated cylindrical fibers perpendicular to the particle motion for both periodic and random distributions. For the case of an isotropic three-dimensional gel made of long fibers, we found the

universal value $a_1 = -2/3$. Since this result was insensitive to the presence of cross-links or randomness in the fiber distribution and that it seems to be valid even when we have tortuous fibers (as long as we keep the distribution isotropic), we believe that it will apply to any realistic gel. Note that this difference ($a_1 = -1$ vs $a_1 = -2/3$) is not only a dimensional one: for example, the case of isolated spherical obstacles in three dimensions gives $a_1 = -1/2$.[23] While the first coefficient (a_1) seems to be independent of the distribution of obstacles, it is not the case for the other coefficients $a_{i\geq 2}$. Even the second coefficient (a_2) is strongly affected by the specific geometry of the gel. For example, changing a simple periodic system to a random distribution or adding some cross-links can make the second coefficient to change its sign. The main assumption in the OMRC model, namely that the low-field mobility is directly proportional to the available volume $f = 1 - \phi$, is thus incorrect. The first coefficient is not, in general, equal to -1, and the higher ones are not equal to 0. However, for three-dimensional gels made of long stiff fibers, a modified relation, $\mu = 1 - 2/3\phi$, seems to be a good approximation, in the low excluded volume limit, for any type of gel.

Acknowledgment. The author thanks the C3.ca organization for computing resources. This work was supported by a Research Grant from the Natural Science and Engineering Research Council (NSERC) of Canada to G.W.S. and by scholarships from the Fonds pour la Formation de Chercheurs et l'Aide à la Recherche (Québec), NSERC, and the University of Ottawa to J.F.M.

References and Notes

(1) Slater, G. W.; Guo, H. L. *Electrophoresis* **1996**, *17*, 977.
(2) Slater, G. W.; Guo, H. L. *Electrophoresis* **1996**, *17*, 1407.
(3) Slater, G. W.; Treurniet, J. R. *J. Chromatogr. A* **1997**, *772*, 41.
(4) Mercier, J.-F.; Slater, G. W. *Electrophoresis* **1998**, *19*, 1560.
(5) Labrie, J.; Mercier, J.-F.; Slater, G. W. *Electrophoresis* **2000**, *21*, 823.
(6) Boileau, J.; Slater, G. W. *Macromolecules*, in press.
(7) Mercier, J.-F.; Slater, G. W. *J. Chem. Phys.* **1999**, *110*, 6050.
(8) Mercier, J.-F.; Slater, G. W. *J. Chem. Phys.* **1999**, *110*, 6057.
(9) Ogston, A. G. *Trans. Faraday Soc.* **1958**, *54*, 1754.
(10) Morris, C. J. O. R. *Protides of the Biological Fluids, 14th Colloquium*; Elsevier: New York, 1967.
(11) Rodbard, D.; Chrambach, A. *Proc. Natl. Acad. Sci. U.S.A.* **1970**, *65*, 970.
(12) Ferguson, K. A. *Metabolism* **1964**, *13*, 985.
(13) Tietz, D. *Advances in Electrophoresis II*, VCH: New York, 1988.
(14) Locke, D. R.; Trinh, S. H. *Electrophoresis* **1999**, *20*, 3331. In this recent theoretical study of the impact of the local variations of the electrical field around nonconducting obstacles, Locke et al. reported that the Ogston assumption should be valid in the limit of very small electrical fields and very dilute media, as well as in media without percolation limits. Similar studies are currently being done by our group and preliminary results indicate that local variations of the electric field do not change the analyte mobility in the low field limit and for an infinitely small analyte (submitted for publication).
(15) Slater, G. W.; Rousseau, J.; Noolandi, J.; Turmel, C.; Lalande, M. *Biopolymers* **1988**, *27*, 509.
(16) Trinh, S. H.; Arce, P.; Locke, D. R. *Transport Porus Media* **1999**, *1395*, 1.
(17) Amsden, B. *Macromolecules* **1998**, *31*, 8382.
(18) Tsai, D. S.; Strieder, W. *Chem. Eng. Commun.* **1986**, *40*, 207.
(19) Schlicht, L.; Ilgenfritz, G. *Physica A* **1995**, *227*, 239.
(20) Saxton, M. J. *Biophys. J.* **1993**, *64*, 1766.
(21) Johansson, L.; Elvingston, C.; Lofroth, J. E. *J. Chem. Phys.* **1993**, *30*, 7471.
(22) Kim, I. C.; Torquato, S. *J. Chem. Phys.* **1992**, *96*, 1498.
(23) Mercier, J.-F.; Slater, G. W. *J. Chem. Phys.* **2000**, *110*, 6057.

MA001544O